Chapter 11
Crop Yield Estimation Using Remote Sensing and Surface Energy Flux Model

Abstract Spatial variability of energy fluxes calls for remote sensing-based approaches for mapping of fluxes, especially for larger areas. Cumulative consumptive use of water by crops can be related to crop yield with the help of remotely sensed data and surface energy balance models. This chapter discusses the use of surface energy balance models and Landsat images for correlating crop yield with latent heat flux. A case study for wheat and soybean fields is also presented. The modeling frame work and correlation of crop yield to spatially mapped latent heat, Bowen ratio, and wetness index is discussed. Net radiation was determined using the Surface Energy Balance Algorithm for Land (SEBAL) procedure. Applying the Two-Source Energy Balance (TSEB) model, surface temperature and latent and sensible heat fluxes were partitioned into vegetative and soil components and estimated at the pixel level. Results show that latent heat flux and Bowen ratio were correlated (positive and negative) to the yield data, respectively. The effect of microtopography on latent heat flux was shown using the wetness index and latent heat relationship. The flux estimation procedure from the SEBAL–TSEB model was useful and applicable to agricultural fields.

Keywords Remote sensing • Latent heat • SEBAL • Two-source model • Surface energy flux • Yield • Landsat • Bowen ratio • Wetness index • Microtopography

11.1 Introduction

Reliable maps of surface energy fluxes are important for assessing surface–atmosphere interactions. Surface energy balance models simulate microscale energy exchange processes between the ground surface and the near ground atmospheric layer level, and they are required by many environmental disciplines including

W. Abtew and A. Melesse, *Evaporation and Evapotranspiration: Measurements and Estimations*, DOI 10.1007/978-94-007-4737-1_11,

hydrology, agronomy, and meteorology. The energy exchange processes are highly spatiotemporal variable and include exchanges of radiative, sensible heat; latent heat; and subsurface heat. The high spatial variability of these fluxes and exchanges will limit point measurements for larger areas.

Methods for estimating energy fluxes from atmospheric measurements range from gross regional estimates to direct measurements of atmospheric gradients or fluxes. The former provides physical bounds over large areas, insensitive to local surfaces, and the latter measures at a single point (Tanner 1988). The estimation of surface energy fluxes using conventional ground-based procedures requires multiple measurements of variables controlling the process and is time, labor, and cost intensive. For large areas, remote sensing approaches are proven to be useful to estimate surface energy fluxes and parameters. Remote sensing provides data useful to estimate surface energy fluxes in the thermal infrared portion of the spectrum.

Remote sensing- and surface energy balance-based approaches are described in details in Chap. 10. One advantage of using remotely sensed data for hydrologic modeling and monitoring is its ability to generate information over large space and time scales, which is very useful for successful model analysis, prediction, and validation.

Surface energy fluxes are related to surface temperature, vegetative properties, and surface emissivities of land surface. For instance, low temperatures of land surface can be indicative of high moisture, irrigated field and/or vegetated cover, and hence latent heat dominance (Bowen ratio < 1). On the other hand, high temperatures can be an indication of the dominance of dry surface, low soil moisture or stressed vegetation, and hence higher sensible heat flux (Bowen ratio > 1). Vegetative properties can significantly affect the energy fluxes and exchange as they affect the surface air temperature gradient. This gradient determines fluxes of sensible heat and exchange of energy. Surfaces having different vegetation cover can have similar surface temperatures due to the difference in the aerodynamic properties of the surfaces (French et al. 2000).

Due to water vapor losses from agricultural fields, evapotranspiration may exhibit large spatial variability depending on the growth stage of crops and health of the vegetation; hence, studies focused at estimating spatial latent heat fluxes (evapotranspiration) of crop fields are very important. This knowledge can help in high-resolution irrigation water management practices.

The yield of many agricultural crops often can be predicted from the amount of water used by the crop in evapotranspiration (ET), which is the combined evaporation from the soil and transpiration by the crop (Hanks 1974). The relationship between yield and ET, called a crop water production function, has been widely and successfully used in various aspects of crop water management. The crop water production function is a mathematic model that reflects the rule of conversion between the crop yield and the water factor (ET). It is widely used in regional planning for improving irrigation efficiency and system evaluation. Based on the crop water production function, relationships between crop yield and consumptive water use have been developed. Such information can be used in crop

water management to determine the amount of water that will result in the highest yield production per unit of water use (water use efficiency). The information from such analysis will be useful to farmers and irrigation managers, as well as to other researchers who investigate methods to increase the productivity and efficiency of crop water use.

11.2 Surface Energy Flux Budget

Surface energy flux estimation requires energy inputs, moisture conditions of soil and vegetation, and surface microclimate conditions (Norman et al. 1995a; French et al. 2000). Remote sensing has proven to provide the energy inputs (short- and longwave radiations) and surface moisture conditions of soil and vegetation (surface temperature and vegetation indices) at a reasonable spatial and temporal scale. Surface microclimate can be collected from networks of meteorological stations.

As shown in Chap. 10, in the absence of horizontally advective energy, the surface energy budget of land surface satisfying the law of conservation of energy can be expressed as

$$R_{\mathrm{n}} - \mathrm{LE} - H - G = 0 \tag{11.1}$$

Energy flux models solve Eq. 11.1 by estimating the different components separately. Remote sensing-based models have proven the ability to address the spatial variability of these fluxes by computing the value of energy budget components in the equation above at pixel level.

As discussed in Chap. 10, the Surface Energy Balance Algorithms for Land (SEBAL) (Bastiaanssen et al. 1998a, b) and the Two-Source Energy Balance (TSEB) (Norman et al. 1995b; Kustas and Norman 1999) models utilize remotely sensed data such as Landsat, ASTER, and MODIS to solve Eq. 11.1 by computing surface energy fluxes from satellite images and meteorological data.

The SEBAL model has been used in various studies to assess evapotranspiration rates in the USA, Spain, Italy, Turkey, Pakistan, India, Sri Lanka, Egypt, Niger, and China (Bastiaanssen et al. 1998a, b; Wang et al. 1998; Bastiaanssen 2000; Morse et al. 2000; Melesse and Nangia 2005; Melesse et al. 2007).

This chapter discusses the use of the coupled SEBAL–TSEB model and Landsat imagery in estimating latent heat fluxes from wheat and soybean agricultural fields and makes comparisons to actual yield of the crop fields. The two models are discussed in detail in Chap. 10.

In order to estimate daily evapotranspiration, instantaneous ET was converted to daily ET using the following equations:

$$\mathrm{ET}_{\mathrm{inst}} = 3600 \frac{\lambda \mathrm{ET}}{\lambda} \tag{11.2}$$

Table 11.1 Coefficients for ASCE-PM Ref-ET equations (Allen et al. 2005)

	Short reference (ET_o)		Short reference (ET_r)			
Computation time step	C_n	C_d	C_n	C_d	Units	Units for R_n, G
Daily or monthly	900	0.34	1,600	0.38	mm day^{-1}	MJ m^{-2} day^{-1}
Hourly – daytime	37	0.24	66	0.25	mm h^{-1}	MJ m^{-2} h^{-1}
Hourly – nighttime	37	0.96	66	1.7	mm h^{-1}	MJ m^{-2} h^{-1}

$$ET_r F = \frac{ET_{inst}}{ET_r} \tag{11.3}$$

$$ET_{24} = ET_r F \times ET_{r24} \tag{11.4}$$

ASCE-PM Standardized Reference ET equation (Jensen et al. 1990) is given by

$$ET_{ref} = 0.408 \frac{\Delta(R_n - G) + \gamma \frac{C_n}{T+273} u_2 (e_s - e_d)}{\Delta + \gamma(1 + C_d u_2)} \tag{11.5}$$

where ET_{ref} is either the short (ET_o) or tall (ET_r) reference ET (mm day^{-1}, or mm h^{-1}), R_n is the net radiation at the crop surface (MJ m^{-2} day^{-1} or MJ m^{-2} h^{-1}), T is the mean daily or hourly temperature at a 1.5–2.5-m height (°C), G is the soil heat flux density at the soil surface (MJ m^{-2} day^{-1} or MJ m^{-2} h^{-1}), u_2 is the mean daily or hourly wind speed at a 2-m height (m s^{-1}), e_s is the mean actual saturation vapor pressure at 1.5–2.5-m height (kPa), e_d is the mean actual vapor pressure at 1.5–2.5-m height (kPa), Δ is the slope of the vapor pressure–temperature curve (kPa $°C^{-1}$), γ is the psychrometric constant (kPa $°C^{-1}$), and C_n is a function of the computation time step (hourly or daily) and of the aerodynamic resistance, which is a function of the reference type: grass or alfalfa. The term C_d is a constant that is a function of the surface resistance values, which are also functions of the reference type: grass or alfalfa. Jensen et al. (2000) gave the values of C_d and C_n as shown in Table 11.1.

11.3 Case Study

The surface energy flux versus crop yield study was conducted for six growing seasons from 1997 to 2002 on four contiguous fields located in Polk County, Northwestern Minnesota (Fig. 11.1). The study fields covering an area of 250 ha (2.5 km^2) are located in the Red River Valley, which is one of the nation's most fertile agricultural areas. Wheat and sugar beets are the most important crops in Polk County. Barley has the second most acreage but stands as the third most economically important crop. The study uses yield and ET data from wheat and soybean fields.

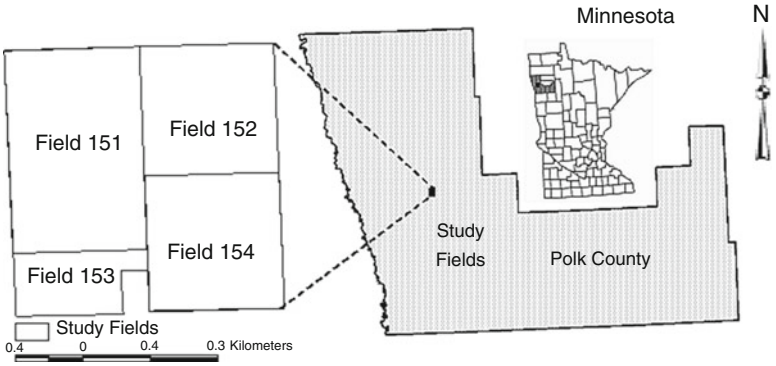

Fig. 11.1 Location of the study fields on the map of Minnesota

Table 11.2 Landsat images used in the study

Date	Sensor	No. of bands	Spatial resolution
June 21, 1997	TM	7	30-m (visible, NIR and MIR), 120-m (TIR)
July 10, 1998	TM	7	30-m (visible, NIR and MIR), 120-m (TIR)
July 21, 1999	TM	7	30-m (visible, NIR and MIR), 120-m (TIR)
July 23, 2000	ETM+	8	30-m (visible, NIR and MIR), 60-m (TIR) panchromatic (15-m)
July 10, 2001	ETM+	8	30-m (visible, NIR and MIR), 60-m (TIR) panchromatic (15-m)
July 13, 2002	ETM+	8	30-m (visible, NIR and MIR), 60-m (TIR) panchromatic (15-m)

The average winter temperature of the area is −13°C with the average daily minimum temperature of −18°C. In summer, the average daily temperature is 20°C with average maximum of 30°C. The total annual precipitation of the area is 505 mm with 70% of the precipitation occurring in the months of April through September. The growing season for most crops falls within this period. The soils in Polk County generally are dark and range in texture from clayey to sandy. Soils in the western half of the county were formed in silty and clayey lacustrine sediments.

11.3.1 Data

The study used remotely sensed data (Landsat Thematic Mapper, TM, and Enhanced Thematic Mapper Plus, ETM+), Digital Elevation Model (DEM), and crop data (yield) and weather data (solar radiation, wind speed, and air temperature).

Seven Landsat TM and ETM + images (Table 11.2) were used to process the intermediate parameters (Normalized Difference Vegetation Index, NDVI), fractional vegetation cover, radiometric surface temperature corrected using surface

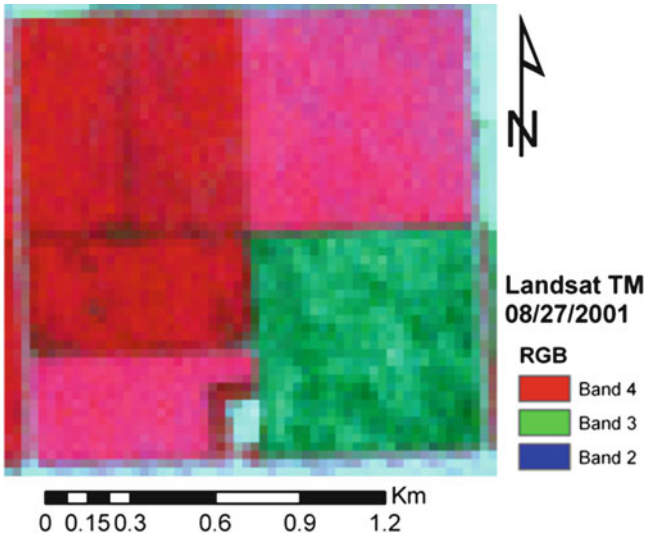

Fig. 11.2 Landsat images of the study area

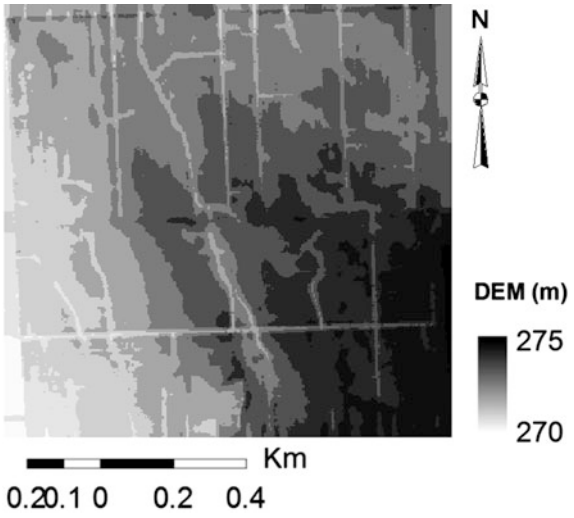

Fig. 11.3 5-m Digital Elevation Model (DEM) of the field

emissivity, albedo, and surface and atmospheric emissivities, from which surface energy flux components were estimated. The Landsat images were selected to represent the growing stage of the crops at full canopy. Figure 11.2 shows one of the Landsat images of the fields used in this analysis.

The 5-m DEM of the field, used in the energy flux computation, was mapped during land preparation (Fig. 11.3). The 5-m yield grids (bushels/acre) for each

Table 11.3 Yield data by season and field

Year	Field 151	Field 152	Field 153	Field 154
1997	Wheat			
1998		Wheat	Soybean	
1999	Wheat		Soybean	
2000		Wheat		Soybean
2001	Soybean			Wheat
2002	Wheat			

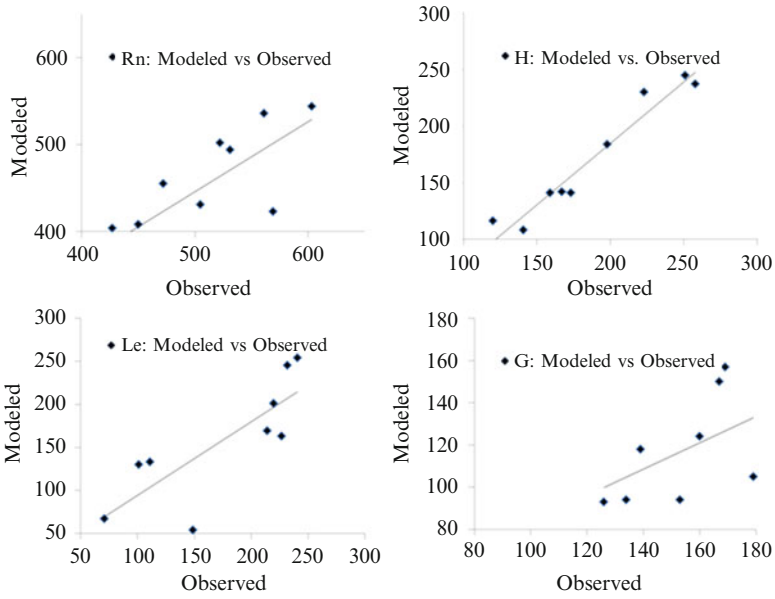

Fig. 11.4 Modeled vs. observed energy fluxes at the Fort Peck, Montana, site

season and field were developed from yield point data collected from the combine harvester's yield monitor. Table 11.3 shows the year and planted crop type by field. Yield data were correlated with the surface energy fluxes determined from the Landsat TM and ETM + sensors.

The weather data, which were used as input to the surface energy flux model, include wind speed and air temperature. Hourly values were collected from the weather station at the study field. Only values at the time of the Landsat overpass of the area were used.

Since the study fields did not have on-site flux measurements, calibration and validation of the modeled fluxes were done using data from the micrometeorology flux tower located at Fort Peck, Montana. Validation results and comparison of the modeled and observed fluxes are shown in Melesse and Nangia (2005). Figure 11.4 shows the comparison of the modeled and predicted fluxes using the SEBAL model at the Fort Peck, Montana, USA, experimental site.

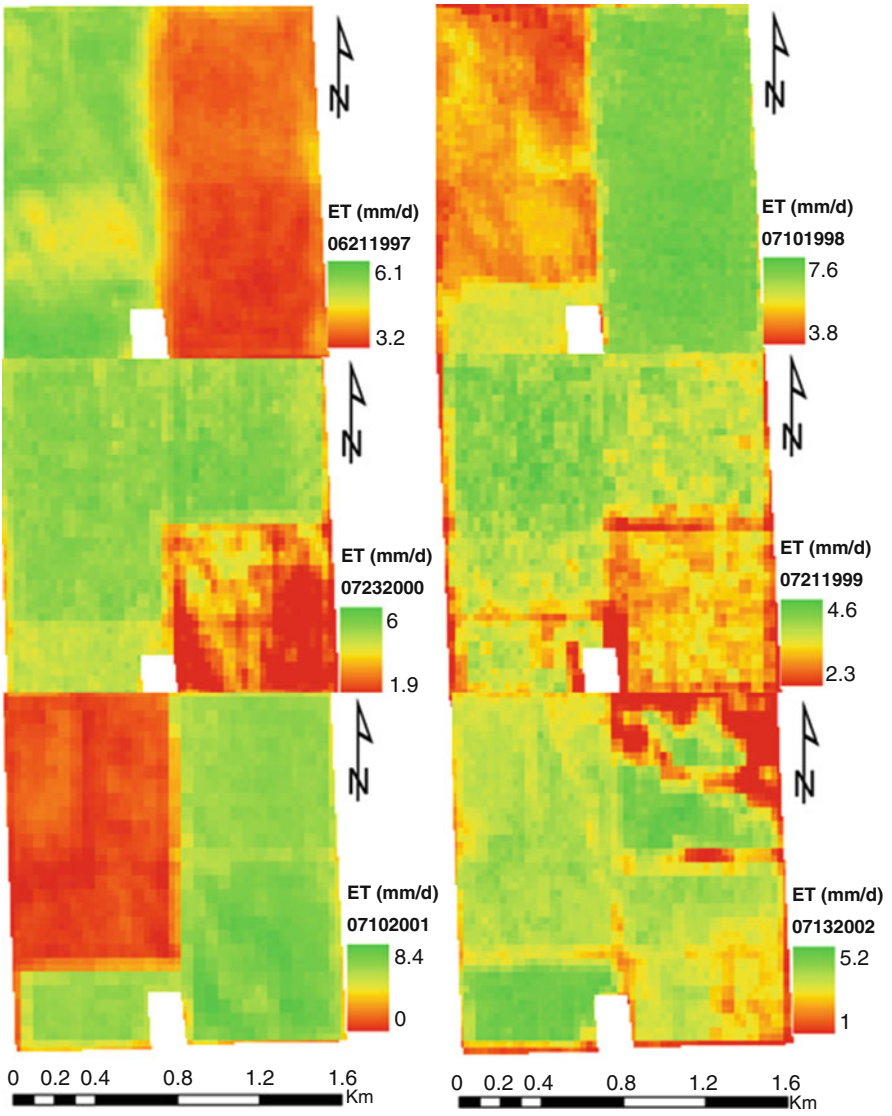

Fig. 11.5 Landsat-based spatial daily evapotranspiration of the study area (1997–2002)

11.3.2 Results and Discussion

Evapotranspiration: Spatial evapotranspiration maps from the six images (1997–2002) are shown in Fig. 11.5. These are daily ET values on the respective image dates. Since the different fields are planted different crops at the different periods, the variation in the spatial and temporal ET emanates from this variation.

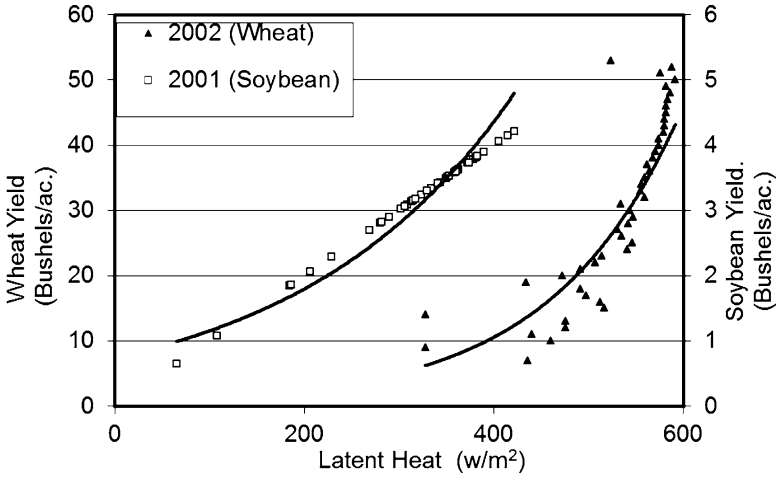

Fig. 11.6 Yield vs. total latent heat (wheat and soybean) from Field 151

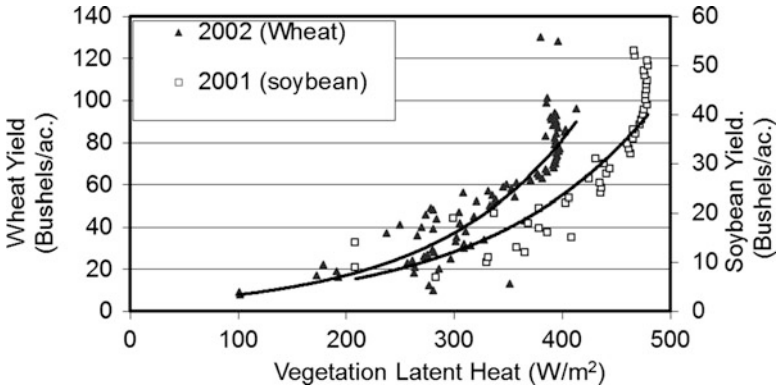

Fig. 11.7 Yield vs. vegetation latent heat (wheat and soybean) from Field 151

Evapotranspiration values in energy units (latent heat flux) were converted to grids and georeferenced to the respective yield grids. Latent heat grids were summarized using integer values of yield grids, and scattergrams were drawn using the mean values of LE for each value of yield. For instance, those latent heat pixels having a yield of 20 bushels/acre were identified, and their mean latent heat value was computed. Scattergrams were drawn using the data categorized by crop (wheat and soybean) and season (2001–2002) for Field 151.

The scattergrams (Figs. 11.6 and 11.7) show that crop yield increases exponentially with the increase of latent heat (total) and vegetative latent heat, with an average R^2 of 0.67 (wheat) and 0.70 (soybean).

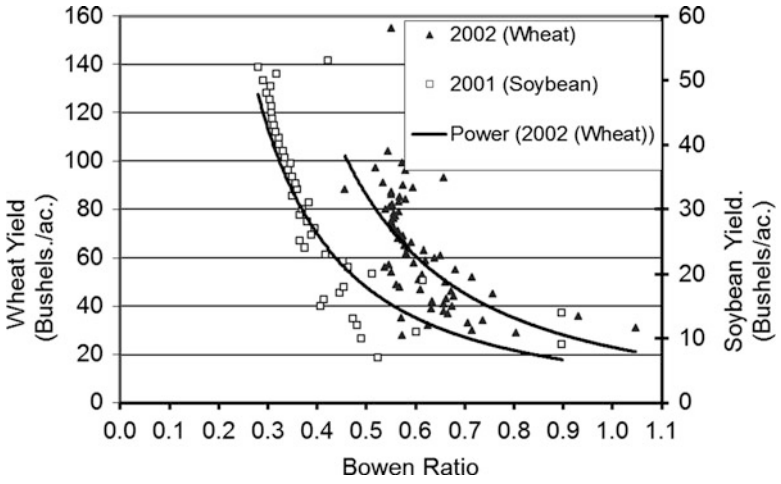

Fig. 11.8 Scattergram showing yield vs. Bowen ratio from Field 151

Yield Versus *Bowen Ratio(Field 151):* The Bowen ratio (B) (Bowen 1926) is computed as the ratio of H to LE. Bowen ratio shows the relative proportions of sensible and latent heat. Higher values of B ($B > 1$) indicate dominance of sensible heat, which is the case for dry soil or stressed vegetation with little evaporation from the soil and reduced respiration from the crop. On the other hand, lower values of B ($B < 1$) are indications of dominance of respiration and evaporation process over sensible heat loss from the soil and canopy to the air. This is typical of a wet soil and vegetated surface. Scattergrams of yield (Fig. 11.8) versus B for Field 151 in the 2001 and 2002 seasons show a negative correlation for both growing seasons, indicating dominance of latent heat flux over the sensible heat from the vegetative surfaces (Fig. 11.8).

Yield Versus *Wetness Index(WI) (Field 151):* Topography is a determinant for magnitudes and spatial distributions of water and energy fluxes over natural landscapes. The topographic configuration of a landscape is a control boundary condition for the hydrologic processes of surface runoff, evaporation, and infiltration, which take place at the ground–atmosphere interface. For example, wetness index (WI) provides a description of the spatial distribution of soil moisture in terms of topographic information. WI is computed as

$$\mathrm{WI} = \mathrm{Ln}\left(\frac{A}{S}\right) \tag{11.6}$$

where A and S are the specific drainage (i.e., flow accumulation) area and slope, respectively.

As A increases and/or S decreases, WI becomes larger, indicating that soil moisture content will increase. Because WI takes into account local slope variations,

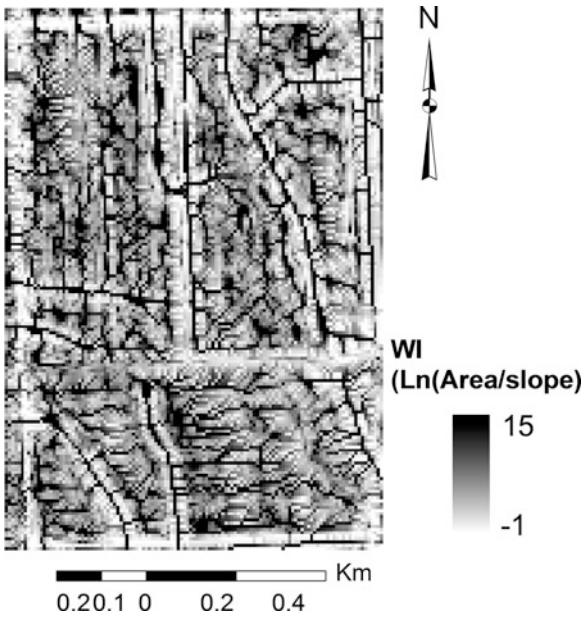

Fig. 11.9 Wetness index (*WI*) of the study area

it has proven to be a reasonable indicator for soil wetness, flow accumulation, saturation dynamic, water table fluctuation, evapotranspiration, soil horizon thickness, organic matter content, pH, silt and sand content, and plant cover density (Kulagina et al. 1995; Florinsky 2000). Wetness index (WI) for the study area is depicted in Fig. 11.9.

The microtopography expressed in the form of the wetness or topographic index and yield from wheat are found to be positively correlated in areas where WI values were low up to a certain extent (Fig. 11.10). This may be because the microtopography controls soil moisture content as well as its spatial distribution. Grids with higher WI values are identified as the areas receiving more overland flows (i.e., with greater flow accumulations) and having a smaller gradient. These areas have higher soil moisture but a higher evaporation rate than the areas with lower WI values. The correlation between WI and soil moisture is further verified by the observation that when water is a limiting factor of an agricultural field, the crop in the areas with higher WI values tends to grow better than the crop in the areas with lower WI values. This can be attributed to more water availability for transpiration (i.e., latent heat demand) in areas with higher WI values. Figure 11.10 shows WI versus yield for wheat and soybean for 2002 and 2001 seasons, respectively. The relation between yield and WI for soybean was not significant.

Yield Prediction ErrorAnalysis: Once the correlation between yield and LE was estimated, a predicted spatial map of yield was generated. In order to show the accuracy of the prediction, the residual mean and standard deviation were calculated (Tables 11.4 and 11.5). From the prediction error analysis, it is shown

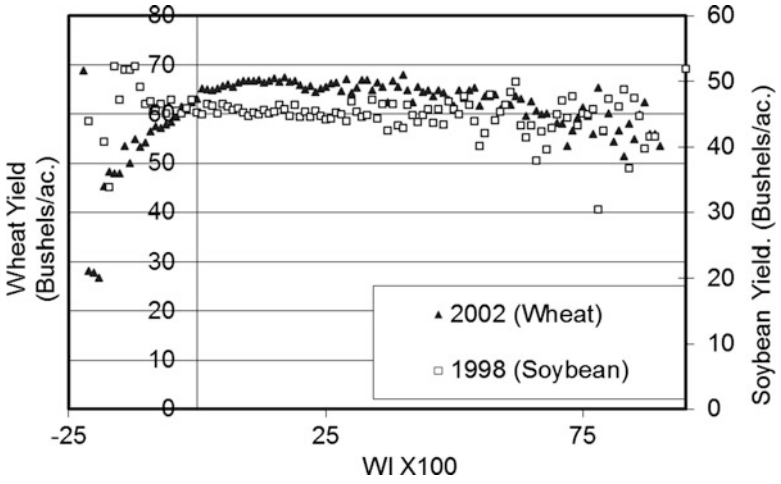

Fig. 11.10 Scattergram showing yield vs. wetness index (*WI*) from Field 151

that the average residual means for wheat and soybean fields were −4.2 and 0.11 bushels/acre, respectively. Similarly, the average standard deviations of the residuals for the wheat and soybean fields were 16.2 and 16.6 bushels/acre, respectively. The error analysis results show that the average error of prediction for soybean fields was smaller than that of the wheat fields. It is also shown that the average percentage of under- or overprediction (ratio of mean residual to observed mean) was also smaller for soybean (1.4%) when compared to wheat (−9.6%).

11.4 Summary

This chapter discussed the role of remotely sensed data and spatially distributed energy flux modeling in estimating evapotranspiration and hence correlating the same to crop yield. The demonstrated case study estimated spatial surface energy fluxes determined from remotely sensed data for seven growing seasons at four crop fields. Energy fluxes were calibrated and verified using flux tower data. Relationships between crop yield to LE, wetness index, and Bowen ratio were established. The SEBAL–TSEB model predicted components of the surface energy budget with reasonable accuracy.

The LE versus yield relationship was good, with an average R^2 of 0.67 for wheat and 0.70 for soybean, respectively. Similarly, the average mean errors of the predicted yield were −0.42 and 1.1 bushels/acre for wheat and soybean, respectively. For developing a better understanding of the close relationships between the LE and crop yield, more data from different fields, crops, and growing seasons will be helpful.

Table 11.4 Mean and standard deviation (SD) of residuals and percent under- or overprediction (% Pred.) of yield by field

	Field 151			Field 152			Field 153			Field 154		
	Residual			Residual			Residual			Residual		
Year	Mean (bu ac^{-1})[a]	SD (bu ac^{-1})	Pred. (%)	Mean (bu ac^{-1})	SD (bu ac^{-1})	Pred. (%)	Mean (bu ac^{-1})	SD (bu ac^{-1})	Pred. (%)	Mean (bu ac^{-1})	SD (bu ac^{-1}	Pred. (%)
1997	−1.99	9.8	−4.7	–	–	–	–	–	–	–	–	–
1998	–	–	–	−4.29	17.51	−8.9	12.68	11.2	37.1	–	–	–
1999	−1.4	8.6	−2.07	–	–	–	−6.73	16.9	−16.5	–	–	–
2000	–	–	–	−5.15	11.62	−23.7	–	–	–	−7.4	31.22	19.6
2001	1.87	7.03	4.77	–	–	–	–	–	–	4.77	28.7	−7
2002	−7.41	20.86	11.27	–	–	–	–	–	–	–	–	–
Average	−2.23	11.57	−3.37	−4.72	14.55	−16.3	2.98	14.1	10.3	6.09	29.96	13.3

[a]1 bushel wheat/soybeans = 27.22 (27) kg and 1 bu/ac wheat/soybeans = 67.25 kg ha^{-1}

Table 11.5 Mean and standard deviation (SD) of residuals and percent under- or overprediction (% Pred.) of yield by crop

	Residuals (all fields)		
Crop	Mean (bu ac^{-1})	SD (bu ac^{-1})	Pred. (%)
Wheat	−4.17	16.19	9.60
Soybean	0.11	16.60	1.42

Acknowledgments The authors acknowledge George Seielstad, Gary Johnson, Ofer Beeri, Grant Casady, David Baumgartner, Santhosh Seelan, Jason Oberg, Chris Carlson, Ganesh Pulicherla, and other members of the Upper Midwest Aerospace Consortium for their help. The authors extend their appreciation to Gary Wagner for providing yield and other field data and Tilden Meyers of NOAA for providing flux tower data for the model validation.

References

Allen RG, Walter IA, Elliott R, Howell T, Itenfsu D, Jensen M (2005). The ASCE Standardized Reference Evapotranspiration Equation. ASCE, Reston, VA

Bastiaanssen WGM (2000) SEBAL-based sensible and latent heat fluxes in the irrigated Gediz Basin, Turkey. J Hydrol 229:87–100

Bastiaanssen WGM, Menenti M, Feddes RA, Holtslag AAM (1998a) A remote sensing surface energy balance algorithm for land SEBAL. 1: formulation. J Hydrol 212–213:198–212

Bastiaanssen WGM, Pelgrum H, Wang J, Ma Y, Moreno J, Roerink GJ, van der Wal T (1998b) The surface energy balance algorithm for land SEBAL. 2: validation. J Hydrol 212–213:213–229

Bowen IS (1926) The ratio of heat losses by conduction and evaporation from any water surface. Phys Rev 27:779–787

Florinsky IV (2000) Relationships between topographically expressed zones of flow accumulation and sites of fault intersection: analysis by means of digital terrain modeling. Environ Model Softw 15:87–100

French AN, Schmugge TJ, Kustas WP (2000) Estimating surface fluxes over the SGP site with remotely sensed data. Phys Chem Earth 25(2):167–172

Hanks RJ (1974) Model for predicting plant yield as influenced by water use. Agron J 66(5): 660–665

Jensen ME, Burman RD, Allen RG (1990) Evapotranspiration and irrigation water requirements, ASCE manual, vol 70. American Society of Civil Engineers, New York

Kulagina TB, Meshalkina JL, Florinsky IV (1995) The effect of topography on the distribution of landscape radiation temperature. Earth Obs Remote Sens 12:448–458

Kustas WP, Norman J (1999) Evaluation of soil and vegetation heat flux predictions using a simple two-source model with radiometric temperatures for partial canopy cover. Agric For Meteorol 94:13–29

Melesse AM, Nangia V (2005) Spatially distributed surface energy flux estimation using remotely-sensed data from agricultural fields. Hydrol Process 19(14):2653–2670

Melesse AM, Nangia V, Wang X, McClain M (2007) Wetland restoration response analysis using MODIS and groundwater data. Special issue: remote sensing of natural resources and the environment. Sensors 7:1916–1933

Morse A, Tasumi M, Allen RG, Kramber W (2000) Application of the SEBAL methodology for estimating consumptive use of water and streamflow depletion in the Bear River Basin of Idaho through remote sensing. Final report submitted to the Raytheon Systems Company, Earth Observation System Data and Information System Project, by Idaho Department of Water Resources and University of Idaho, 107 pp

Norman JM, Divakarla M, Goel NA (1995a) Algorithms for extracting information from remote thermal-IR observations of the earth's surface. Remote Sens Environ 51:157–168

Norman JM, Kustas WP, Humes KS (1995b) A two-source approach for estimating soil and vegetation energy fluxes from observations of directional radiometric surface temperature. Agric For Meteorol 77:263–293

Tanner B (1988) Use requirements for Bowen ratio and eddy correlation determination of evapotranspiration. In Proceedings of the specialty conference of the irrigation and drainage division. ASCE, Lincoln, NE, 19–21, July, 1988

Wang J, Bastiaanssen WGM, Ma Y, Pelgrum H (1998) Aggregation of land surface parameters in the oasis-desert systems of Northwest China. Hydrol Process 12:2133–2147